Defects in codoped NiO with gigantic dielectric response

Ping Wu,* Valeri Ligatchev, Zhi Gen Yu, Jianwei Zheng, Michael B. Sullivan, and Yingzhi Zeng
Institute of High Performance Computing, 1 Fusionopolis Way, No. 16-16 Connexis, Singapore 138632, Singapore
(Received 10 May 2009; published 16 June 2009)

We combine first-principles, statistical, and phenomenological methods to investigate the electronic and dielectric properties of NiO and clarify the nature of the gigantic dielectric response in codoped NiO. Unlike previous models which are dependent on grain-boundary effects, our model based on small polaron hopping in homogeneous material predicts the dielectric permittivity (10^{4-5}) for heavily Li- and M_D-codoped NiO (M_D =Ti, Al, Si). Furthermore, we reproduce the experimental trends in dielectric properties as a function of the dopants nature and their concentrations, as well as the reported activation energies for the relaxation in Li- and Ti-codoped NiO (0.308 eV or 0.153 eV depending on the Fermi-level position). In this study, we demonstrate that small polaron hopping on dopant levels is the dominant mechanism for the gigantic dielectric response in these codoped NiO.

DOI: 10.1103/PhysRevB.79.235122 PACS number(s): 71.20.Be, 71.15.Mb, 71.55.Ht, 77.22.−d

Nickel oxide (NiO) with a band gap of 3.7–4.3 eV is a prototypical charge-transfer insulator,[1] whose astonishing macroscopic properties and electron spectrum are usually attributed to strong electron-electron correlations in 3d shells.[2] Its dc conductivity σ_{dc} of less than 10^{-13} S/cm can be increased by 15 orders of magnitude through doping of monovalent ions such as Li^{+}.[3,4] The Li acceptor energy level is about 0.15 eV above the valence-band maximum (VBM), which results in a very high hole concentration of approximately 10^{19} cm^{-3}.[5] Recently, NiO-based compounds codoped with monovalent [Li^{+},[6,7] K^{+},[8,9] and Na^{+} (Ref. 10)] and trivalent or tetravalent [Al^{+3},[11] Si^{+4},[12–14] Ta^{+4},[15] Ti^{+4},[6,7] and Zr^{+4} (Ref. 16)] dopants have attracted immense scientific interest due to their unusually high ($\sim 10^4 - 10^6$ at room temperature) real part of the complex dielectric permittivity $\varepsilon^*(\omega,T) = \varepsilon'(\omega,T) - i\varepsilon''(\omega,T)$,[17] which may allow for new applications in microelectronics and energy-storage devices. Currently, the exact origin of the gigantic dielectric permittivity and general guidelines for the selection of dopants are still not firmly established. Existing models like the Maxwell-Wagner (MW) model[18] attributes the high dielectric permittivity predominantly to drastic microstructure nonhomogeneities.[6,7] In general, it allows one to estimate $\varepsilon^*(\omega,T)$ magnitude but not its frequency and temperature dependencies. More importantly, the majority of basic parameters in the MW model cannot be introduced self-consistently or satisfactorily; for instance, the grain-boundary (GB) width t and dielectric permitivity $\varepsilon_{\mathrm{GB}}$ are not established reliably even for the most studied case of Li- and Ti-codoped NiO (LTNO). Indeed, t of "few nanometers" and $\varepsilon_{\mathrm{GB}} = 10 - 50$ were claimed,[6] while $t = 30$ nm, and $\varepsilon_{\mathrm{GB}} = 50$ were suggested.[7] Our estimations of GB width based on the "sharp" p-n junction model results in $t < 2.7$ nm at $\varepsilon_{\mathrm{GB}} = 50$ and dopant concentrations of 10^{21} cm^{-3}, implying strong under-barrier tunneling, which reduces the GB effects. Furthermore, no strong correlation between $\varepsilon'(\omega,T)$ magnitude and grain size D has been reported so far. The absence of such correlations was clearly shown: D in the LTNO-850 sample (15.7 ± 2.3 μm) is larger than that of the LTNO-900 sample (14.7 ± 2.1 μm) though $\varepsilon'(\omega,T)$ quantity for the first sample is lower.[7] In addition, $\varepsilon'(\omega,T)$, of the Li, Fe codoped NiO and Li, V codoped (LVNO) samples are nearly the same despite the drastic differences in the grain sizes: 3.3 ± 0.9 and 46 ± 14 μm were obtained for those LFNO and LVNO materials, respectively.[19] At the same time, dielectric permittivity for both aforementioned ceramics considerably exceeds that for LTNO sample with the grain sizes of 4.8 ± 2.0 μm.[19] All grain sizes mentioned above have been evaluated using scanning electron microscopy (SEM) images; however, they do not match those sizes obtained by other experimental methods. In particular, the analysis of x-ray diffraction data has suggested grain sizes just from 39 to 72 nm (i.e., 200–250 times smaller than on SEM images) for LTNO samples.[7] Finally, very recent experimental data clearly show dominant "electrical response inside the grains," while the GB role is fairly insignificant.[19] All these greatly weaken the physical background for any nonhomogeneity-based gigantic dielectric response mechanism, including the MW model. In this study, a combination of first-principles, statistical, and phenomenological methods are employed to investigate the electronic and dielectric properties of NiO and clarify the nature of the gigantic dielectric response in codoped NiO.

Starting from first-principles calculations, we evaluate the dopant formation energy E_f as well as its energy level in the NiO forbidden gap. In NiO, the E_f of a dopant (M) was calculated as a function of the Fermi energy E_F,

$$E_f = E^{\mathrm{def}} - n_{\mathrm{Ni}}\mu_{\mathrm{Ni}} - n_{\mathrm{O}}\mu_{\mathrm{O}} - n_M\mu_M + qE_F, \tag{1}$$

where E^{def} is the total energy of NiO supercell containing a defect. $n_{\mathrm{Ni,O},M}$ and $\mu_{\mathrm{Ni,O},M}$ are the number and the chemical potential of Ni, O, and dopant element M, respectively, q is the charge of the dopant-related defect or Ni vacancy in NiO. All possible charged states of the substitutional defects (M_{Ni}) and Ni vacancy (V_{Ni}) are considered. Density-functional-theory-based calculations are performed using the VASP code[20] within the local-spin-polarized density approximations (LSDA+U,[21] U_{eff}=5.3 eV). Projector augmented wave pseudopotentials[22] and a $2\times2\times2$ k-point sampling in a $3\times3\times3$ supercell with a plane-wave basis cutoff energy of 400 eV were used in our calculations.

The chemical-potential ranges of Eq. (1) are determined by the thermodynamic conditions. For NiO, at equilibrium,

 ©2009 The American Physical Society

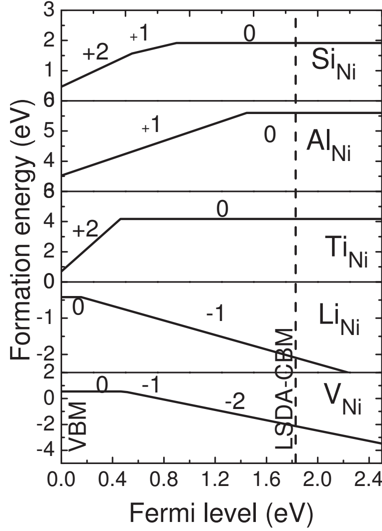

FIG. 1. The formation enthalpies of Ni vacancy and M dopant as a function of Fermi level in NiO under the oxygen-rich condition ($\mu_O = \frac{1}{2}\mu_{O_2}$). The charged states of q are denoted by number, whereas the transition energies $\varepsilon(q/q')$ are the kinks of each line. The VBM is set to zero and the dashed line indicates the LSDA conduction-band minimum.

we have $\mu_{Ni}+\mu_O=\Delta H_f^{NiO}$, where ΔH_f is the compound enthalpy relative to O_2 and solid metallic Ni. In order to avoid the formation of competing phases (i.e., element solids Ni and M dopants, the O_2 gas, and the compounds Li_2O, TiO_2, Al_2O_3, and SiO_2), the chemical potential should be constrained to $\mu_i \le 0$ $(i=Ni,Li,Ti,Al,Si,O)$, $2\mu_{Li}+\mu_O \le \Delta H_f^{Li_2O}$, $\mu_{Ti}+2\mu_O \le \Delta H_f^{TiO_2}$, $2\mu_{Al}+3\mu_O \le \Delta H_f^{Al_2O_3}$, and $\mu_{Si}+2\mu_O \le \Delta H_f^{SiO_2}$. The calculated formation energy enthalpies are −2.38(−2.48), −6.58(−6.17), −2.37(−2.57), −18.29(−17.37), and −9.94(−9.14) eV for NiO, Li_2O, TiO_2, Al_2O_3, and SiO_2, respectively, which match well to experimental values given in parentheses. Based on the reported experiments,[6,12,23] we fixed the O chemical potential as $\mu_O = \frac{1}{2}\mu_{O_2}$, and the chemical potentials of Ni and M dopants are calculated under the above constrains. Therefore, we obtained the formation enthalpies for V_{Ni} and M_{Ni} based on Eq. (1). The effect of oxygen chemical potential will not be discussed in this work.

The formation enthalpies of V_{Ni} and M dopant in NiO are shown in Fig. 1. Meanwhile, we evaluate the thermal transition-energy levels (TRLs) $\varepsilon(q/q')$ relative to the VBM, which is defined as the Fermi-level position where both charged states of q and q' have the same formation energy as shown in Table I. It was found that V_{Ni} and Li_{Ni} have the lowest formation enthalpy with corresponding TRLs of 0.515 and 0.153 eV, respectively. The calculated V_{Ni} and Li_{Ni} acceptor levels are very close to the experimentally reported

TABLE I. Calculated $\varepsilon(q/q')$ of Ni vacancy and M dopant in NiO (eV).

	V_{Ni}	Li_{Ni}	Ti_{Ni}	Al_{Ni}	Si_{Ni}
$\varepsilon(q/q')$	0.515	0.153	0.461	1.446	0.897

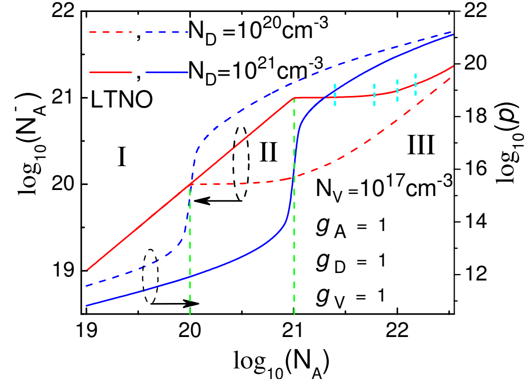

FIG. 2. (Color online) Dependencies of concentrations (cm^{-3}) of the electrically active acceptors (left axis) and free holes (right axis) on the total concentration of Li dopants in LTNO material at room temperature with two different concentrations of donors: 10^{20} and 10^{21} cm^{-3}. Vertical dashed lines mark out $N_A=N_D$ equality. Dotted lines indicate concentrations of Li_{Ni} corresponding to experimental points from Ref. 6.

results of 0.4–0.7 eV and is 0.1–0.2 eV,[24] respectively. The values are consistent with other theoretical predictions.[5]

Occupancies of the aforementioned defect levels can be evaluated within the framework of standard (i.e., without onsite correlation effects) equilibrium statistics of a hole gas in a semiconductor[25] by using a condition of charge neutrality for a material with impurity levels placed predominantly in the lower part of the band gap

$$N_D^+ + p = N_A^- + N_V^-, \tag{2}$$

where $N_{D,A,V}^{+/-}$ is volume concentration of ionized donor, acceptor, and nickel vacancy, respectively, p is the volume concentration of free holes in VB. The concentration of free electrons n in the conduction band should be negligible for such a case.

Figure 2 shows $\log_{10}(N_A^-)$ vs $\log_{10}(N_A)$ and $\log_{10}(p)$ vs $\log_{10}(N_A)$ curves at room temperature and with two different donor concentrations (10^{20} and 10^{21} cm^{-3}) for LTNO. In Fig. 2, N_A^- vs N_A dependencies can be divided into three regimes. In regime I ($N_A \ll N_D$), N_A^- vs N_A remains linear with a unity slope (regardless particular N_D quantity); however it "saturates" sharply in regime II ($N_A \approx N_D$), though N_A^- starts to grow again at regime III ($N_A \gg N_D$), i.e., when $N_A \cong 5-10 \times N_D$. In regime II (which corresponds to a case of "compensated semiconductor"), concentrations of free holes rise abruptly (about 4 to 5 orders of magnitude at room temperature). When $N_A \ll N_D$ (regime I), charge balance in the Li^--, Ti^--, and codoped NiO corresponding to a predominantly n-type semiconductor; however, when $N_A \gg N_D$ (regime III), the material becomes predominantly p type with a high concentration of VB free holes (Fig. 2) and, consequently, pronounced p type of dc conductivity. On the other hand, N_A^- vs N_A dependencies are not greatly effected by large changes in concentration N_V ($10^{17}-10^{21}$ cm^{-3}) nor level degeneracies.

The simulated effects of N_A and N_D on room-temperature E_F level in LTNO are illustrated in Fig. 3. It is found that E_F lies near (at E_{F-V}=0.07–0.08 eV) the VBM when $N_A \gg N_D$

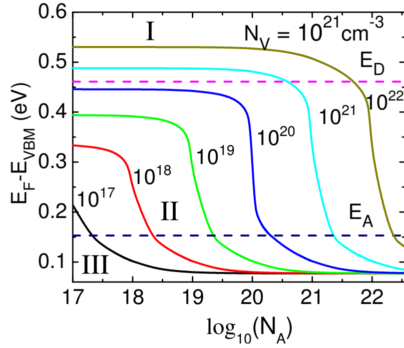

FIG. 3. (Color online) Simulated room-temperature dependencies of Fermi-level positions relative to $E_{\rm VBM}$ (E_{F-V}) on the total concentration of Li (cm^{-3}) dopant in the NiO-based compound, codoped with Ti at six different concentrations (shown in the figure in cm^{-3} next to the corresponding curve). Dashed horizontal lines correspond to Li acceptor and Ti donor levels.

(regime III, i.e., in LTNO, predominantly doped with Li), while E_{F-V}=0.45–0.53 eV at $N_A \ll N_D$ (regime I, i.e., in LTNO, predominantly doped with Ti). The area where E_{F-V}=0.20–0.40 eV corresponds to the case $\log_{10}(N_A) \approx \log_{10}(N_D)$ (regime II), i.e., in the compensated LTNO. For such intermediate positions of Fermi level, acceptor level is almost completely occupied and negatively charged, while positively charged donor states are largely empty due to electron-hole transitions from Ti- to Li-related centers. Consequently, the activation energy of the polarization at the intermediate E_F positions equals to $E_D - E_A$=0.308 eV, which is in very good agreement with the experimentally observed activation energy of 0.313 eV (Refs. 6 and 23) for the polarization in LTNO. The latter activation-energy magnitude is also close to the experimental data from Ref. 19, where *intragranular* activation energy of 0.293 eV has been deduced for LTNO (i.e., within accuracy of 5% with corresponding our simulation result). However, when the concentration of Li-related acceptor centers clearly dominates over Ti-related donor ones (regime III, $N_A \gg N_D$), the E_F position shifts toward the VBM below the E_A level (Fig. 3); as a result, the activation energy is now determined by the position of acceptor energy level, which equals 0.153 eV (Table I), and matches very well again to the experimental activation energy of 0.14–0.18 eV for dc conductivity in heavily Li-doped LTNO.[7,26]

NiO is a classic material with a small polaron transport.[27] Therefore, the real part $\varepsilon'(\omega)$ of the $\varepsilon^*(\omega)$ function of heavily codoped LTNO can be evaluated within the framework of polaron hopping model, which predicts the Drude-type low-frequency $[\omega \ll \omega_p = (4\pi n e^2 \tau / m\varepsilon')^{1/2}]$ dielectric response of the many-body normal-state polaron system.[28] In our study, we use the following modification of the Drude formula:

$$\varepsilon'(\omega) = \varepsilon_m [1 - n e^2 \tau(\omega)/(m^* \omega)], \qquad (3)$$

where ε_m is the relative permittivity of the matrix, n is the concentration of polarons, e the is the elementary charge, $\tau(\omega)$ is the relaxation time (frequency dependent in general), and m^* is the effective mass of the polarons. In accordance to the Prins model, the majority of "electrically active" charge carriers in LTNO (especially at "intermediate" E_F position) is located at "defect" states created due to the presence of dopants. Thus, polaron hopping predominately occurs on E_A, E_D, and VBM levels. Typically, $\tau = 8.47 \times 10^{-13} - 1.32 \times 10^{-11}$ s was reported in codoped materials.[6,8] Applying Eq. (3), we obtained $\varepsilon'(\omega) \cong 3.8 \times 10^4$ at $\varepsilon_m = 10$, $\omega = 2\pi \times 1000$ Hz, $n = N_A^- = N_D^+ = 10^{21}$ cm^{-3}, $\tau = 8.47 \times 10^{-13}$ s, and $m^* = 1.247 m_0$ (with an electron-phonon coupling constant of 1.26) in excellent agreement with experimental $\varepsilon'(\omega)$ values revealed in Fig. 2(a) of Ref. 6. As seen from that figure, the frequency dependencies $\varepsilon'(\omega)$ measured on codoped NiO are quite complicated though a declining trend is typical for these dependencies.[6,7] Such $\varepsilon'(\omega)$ behavior is readily explainable in our generalized [i.e., with frequency-dependent $\tau(\omega)$ term] model, if we assume $\tau(\omega) = A\omega^S$, which eventually yields a generic (for hopping mechanisms) $\varepsilon'(\omega) \sim \omega^{S-1}$ behavior with the parameters A and S depending further on the features of the polarons hopping. ac hopping conductivity $\sigma(\omega)$ with the archetypal frequency dependence $\sigma(\omega) \sim \omega^S$ (S =0.80–0.96) was reported for many solid-state systems and corresponding theoretical models were studied extensively.[29] In our model, the aforementioned range of the S parameter provides an appropriate slope of the $\varepsilon'(\omega)$ frequency dependence reported in experiments. In particular, we evaluated the slope of $\varepsilon'(\omega)$ dependence on a $\log_{10}$-$\log_{10}$ scale of Fig. 2(a) in Ref. 6 to be $\sim 0.136 \pm 0.009$ at T=310 K. Importantly, our approach is also in line with the universal dielectric response (UDR) model,[30] which essentially is based on an assumption of key contribution to dielectric-response function from the localized charge carriers. UDR also provides an appropriate $\log_{10}$-$\log_{10}$ slope for $\varepsilon'(\omega)$ dependence based on the archetypal dependence for $\sigma(\omega)$.

Our model can be used to explain the effects of Li and Ti concentrations on the dielectric permittivity of LTNO reported in Ref. 6 (see Fig. 4 therein). They observed room-temperature $\varepsilon'(\omega, T)$ quantity increased (decreased) with increasing Li (Ti) concentration when $N_{\rm Li} > N_{\rm Ti}$ ($N_{\rm Li} < N_{\rm Ti}$). $N_{\rm Li} > N_{\rm Ti}$ corresponds to $N_A > N_D$, i.e., regime III in Fig. 2. We show the concentrations of Li corresponding to experimental points in Fig. 4 of Ref. 6 with short vertical-dashed cyan lines. In regime III, the position of the Fermi level is situated in between VBM and the acceptor level (Fig. 3). Thus, intensive small polaron hopping can be expected in this regime both at E_A and VBM levels. This additional contribution would eventually result in the $\varepsilon'(\omega, T)$ enlargement with the N_A. In particular, ε' dependencies versus the level of codoping with Li is expected to exhibit a general shape similar to that of N_A^- vs N_A function in Fig. 2 (regime III) with $\varepsilon'(\omega, T) \cong 3.8 \times 10^4$ at $N_A \cong 10^{21}$ cm^{-3}, $\varepsilon'(\omega, T) \cong 4.8 \times 10^5$ at $N_A \cong 5 \times 10^{22}$ cm^{-3} (all these quantities correspond to T =300 K, $N_D = 10^{21}$ cm^{-3}, and $\omega = 2\pi \times 1000$ Hz). An increase in Ti concentration causes E_F to increase toward the acceptor level; this shift initially (i.e., when $E_F < E_A$) yields an increase in the occupations of the acceptor states and a corresponding reduction in polaron hopping (especially at VBM) and polarization processes. When $N_{\rm Ti}$ is larger than $N_{\rm Li}$ (regime I), E_F overcomes E_A level, yielding an abrupt enlargement in the activation energy of the polarization [which is now determined by $E_D - E_A$ interval and equals to

0.308 eV for LTNO (Fig. 3)], exponential deduction of the defect-level occupation, and sharp $\varepsilon'(\omega,T)$ diminishment. To further support our model, we correlate the first-principles-simulated donor levels of Si and Al (Table I) and real part of the dielectric permittivity for Li, Al- and Li, and Si- codoped NiO ceramics: wider E_D-E_A interval (0.744 and 1.293 eV for Si and Al codopants, respectively) usually yields a significantly lower $\varepsilon'(\omega,T)$ of 10^3-10^4 for both Al- and Si-codoped NiO:Li (Ref. 11) compared to 4×10^4 for LTNO.

The high dielectric loss in NiO-based ceramics can also be explained by this mechanism. Based on the standard relation $\sigma_{dc}=e\mu_p p$, and assuming $\mu_p=0.3$ cm^2 V^{-1} s^{-1},[31] we can expect $\sigma_{dc}=4.81\times10^{-7}$ S/cm at $p=10^{13}$ cm^{-3} (which corresponds in Fig. 2 to N_A value slightly below the "critical" value of 10^{21} cm^{-3}), and $\sigma_{dc}=4.81\times10^{-2}$ S/cm at $p=10^{18}$ cm^{-3} (which corresponds in Fig. 2 to an N_A magnitude slightly higher than the critical value of 10^{21} cm^{-3}) at $T=300$ K. For comparison, a nominally undoped silicon has $\sigma_{dc}=3.1\times10^{-6}$ S/cm at $T=300$ K.[32] Considering only dc conductivity contribution to dielectric loss, we have $\varepsilon''_{dc}(\omega,T)\cong0.09$ at $p=10^{13}$ cm^{-3}, but $\varepsilon''_{dc}(\omega,T)\cong8.65\times10^3$ at $p=10^{18}$ cm^{-3} for $\omega=2\pi\times10^3$ Hz and room temperature. The latter value matches reasonably well to corresponding experimental data.[6,7]

In conclusion, we used a combination of methods to study electronic and dielectric responses in codoped NiO. None of these approaches assumes spatial heterogeneity of codoped NiO materials. The dramatic increase in the dielectric permittivity of codoped NiO compounds with clear Li domination is caused by VB polarons but at the expense of high dielectric losses. Our model also explains the experimentally observed trends with regard to changes in Li and Ti concentrations. This model is applicable as well for other NiO-based compounds with gigantic dielectric response.

The authors thank Shengbai Zhang from RPI and Leonard J. Brillson from OSU for their very helpful discussions.

*wuping@ihpc.a-star.edu.sg

[1] J. Kunes, V. I. Anisimov, S. L. Skornyakov, A. V. Lukoyanov, and D. Vollhardt, Phys. Rev. Lett. **99**, 156404 (2007).
[2] S. Hüfner, Adv. Phys. **43**, 183 (1994).
[3] V. Biju and M. Abdul Khadar, Mater. Res. Bull. **36**, 21 (2001).
[4] W. Shin and N. Murayama, Mater. Lett. **45**, 302 (2000).
[5] S. Lany, J. Osorio-Guillen, and A. Zunger, Phys. Rev. B **75**, 241203(R) (2007).
[6] J. B. Wu, C.-W. Nan, Y. H. Lin, and Y. Deng, Phys. Rev. Lett. **89**, 217601 (2002).
[7] S. Maensiri, P. Thongbai, and T. Yamwong, Acta Mater. **55**, 2851 (2007).
[8] P. K. Jana, S. Sarkar, and B. K. Chaudhuri, Appl. Phys. Lett. **88**, 182901 (2006); J. Phys D: Appl. Phys. **40**, 556 (2007).
[9] P. K. Jana, S. Sarkar, S. Karmakar, and B. K. Chaudhuri, J. Appl. Phys. **102**, 084105 (2007).
[10] P. K. Jana, S. Sarkar, H. Sakata, T. Watanabe, and B. K. Chaudhuri, J. Phys. D **41**, 065403 (2008).
[11] Y. H. Lin, J. F. Wang, L. Jiang, Y. Chen, and C. W. Nan, Appl. Phys. Lett. **85**, 5664 (2004).
[12] R. Zhao, Y.-H. Lin, X. Zhou, M. Li, and C.-W. Nan, J. Appl. Phys. **100**, 046102 (2006).
[13] Y. Lin, L. Jiang, R. Zhao, G. Liu, and C.-W. Nan, J. Phys. D **38**, 1615 (2005).
[14] Y. Lin, L. Jiang, R. Zhao, and C.-W. Nan, Phys. Rev. B **72**, 014103 (2005).
[15] Y.-J. Hsiao, Y.-S. Chang, T.-H. Fang, Y.-L. Chai, C.-Y. Chung, and Y.-H. Chang, J. Phys. D **40**, 863 (2007).
[16] K. Chen, S. Yuan, P. Li, F. Gao, J. Liu, G. Li, A. Zhao, X. Lu, and J. Zhu, J. Appl. Phys. **102**, 034103 (2007).
[17] K. C. Kao, *Dielectric Phenomena in Solids* (Elsevier, New York, 2004).
[18] Y. Zhu, J. C. Zheng, L. Wu, A. I. Frenkel, J. Hanson, P. Northrup, and W. Ku, Phys. Rev. Lett. **99**, 037602 (2007).
[19] P. Thongbai, S. Pongha, T. Yamwong, and S. Maensiri, Appl. Phys. Lett. **94**, 022908 (2009).
[20] G. Kresse and J. Hafner, Phys. Rev. B **48**, 13115 (1993); **49**, 14251 (1994).
[21] A. I. Liechtenstein, V. I. Anisimov, and J. Zaanen, Phys. Rev. B **52**, R5467 (1995).
[22] G. Kresse and D. Joubert, Phys. Rev. B **59**, 1758 (1999).
[23] Y.-H. Lin, M. Li, C.-W. Nan, J. Li, J. Wu, and J. He, Appl. Phys. Lett. **89**, 032907 (2006).
[24] N. Tsuda, K. Nsau, A. Fujimori, and K. Siratori, *Electronic Conduction in Oxides* (Springer-Verlag, Berlin, 2000), p. 218.
[25] J. F. Prins, Phys. Rev. B **39**, 3764 (1989).
[26] S. van Houten, J. Phys. Chem. Solids **17**, 7 (1960).
[27] D. P. Snowden and H. Saltsburg, Phys. Rev. Lett. **14**, 497 (1965).
[28] A. S. Alexandrov, Phys. Rev. B **46**, 2838 (1992).
[29] P. Lunkenheimer, V. Bobnar, A. V. Pronin, A. I. Ritus, A. A. Volkov, and A. Loidl, Phys. Rev. B **66**, 052105 (2002).
[30] N. F. Mott and E. A. Davis, *Electronic Processes in Non-Crystalline Materials* (Oxford University Press, London, 1971), p. 368.
[31] S. J. Handley and G. W. Bradberry, Phys. Lett. **40**, 277 (1972).
[32] M. Levinstein, S. Rumyantsev, and M. Shur, *Handbook Series on Semiconductor Parameters* (World Scientific, London, 1996), Vol. 1.